DEVELOPMENT OF HYDROPHOBIC CAPILLARY BARRIERS FOR LANDFILL COVERS SYSTEM: ASSESSMENT OF WATER REPELLENCY AND HYDRAULIC PROPERTIES OF WATER REPELLENT SOILS

Shaphal SUBEDI [1)], Shoichiro HAMAMOTO [1)], Toshiko KOMATSU [1)], and Ken KAWAMOTO[1)]
[1)] Soil Mechanics Lab., Department of Civil and Environmental Engineering, Saitama University

ABSTRACT

This study investigated hydrological processes and parameters (with focus on magnitude and time-dependency of water repellency and its controls on water retention and infiltration in hydrophobized porous media) and developed measurement technologies (combining coil-TDR and tensiometer methods for simultaneously determining soil moisture and matric potential) that are essential for the potential design and reliable use of hydrophobized capillary barrier systems. The hydrophobized sands revealed good performance evaluated by measured contact angle and hydraulic properties (soil-water retention curves), implying a good potential for using this techniques in capillary barrier systems. The new mini T-TDR probe thereby seems highly useful for obtaining simultaneous, small-scale (point-like) measurements of water content and matric potential in unsaturated porous media hereunder will facilitate investigating the effects of water repellency (WR) on water retention properties. Moreover, WR had a direct and predictable effect on the soil-water retention curves, and affects the shape of the wetting front.

KEYWORDS: Capillary barrier, hydrophobized sand, water repellency, time domain reflectometry, water retention

1. INTRODUCTION

A capping system is the final component in the construction of engineered sanitary landfills. The proper design of such a system is essential to minimize water percolation into the underlying waste and to control landfill gas emissions. To assure adequate long-term performance, various types of capping systems have been developed to fulfill regulatory standards, including highly technical and expensive systems such as geomembranes and geosynthetic clay liners (Simon and Müller, 2004). Although modern engineered capping systems are technically effective, they do not provide a feasible solution for landfills located in developing countries due to economic and technical constraints, as shown in Table 1.

Recently, earthen covers such as capillary barriers (CBs) and evapotranspirative covers have been proposed as technically feasible and low-cost solutions for limiting water infiltration and controlling seepage at solid waste landfills. The CBs can be constructed in various designs, typically consisting of a fine-grained layer overlying a coarser grained layer (Stormont, 1995). In evapotranspirative covers, there is no increase in storage capacity, rather water uptake by plants and evapotranspiration (ET) prevents deep percolation. The evapotranspirative covers can be used not only as monolithic ET covers, but also as capillary barrier ET covers, and anisotropic barrier ET covers in combination with CBs (Albright et al., 2003).The earthen cover systems have proved to be effective for landfills located in semiarid and arid regions (Benson and Khire, 1995; Sharma and Reddy, 2004). Their application in wet regions can be problematic, however, because under high-precipitation events, their impermeable properties may be compromised in the long term (Koerner and Daniel, 1997).

In developing the concept of “hydrophobic capillary barriers”, one of the possible techniques to enhance the impermeable properties of capillary barrier is to make soil grain surfaces water repellent by mixing or coating the earthen cover materials with low-cost and locally available hydrophobic agents (HAs). The concept of “hydrophobic capillary barrier” is expected to perform well and to be applicable for arid, semi arid and wet weather conditions. The hydrophobized capillary barrier is formed by two layers, typically consisting of erosion layer overlying a hydrophobized sand layer (Fig. 1). The

erosion layer should be graded at a slope between 2-5% (Sharma and Reddy, 2004), and capable of supporting vegetation and preventing cracking, freezing, or other damage to the lower hydrophobized barrier layer. Gravel is placed below the hydrophobized barrier capping layer to reduce the differential settlement that may be caused by irregular surface. Moreover, it can be constructed to form a gas collection layer, depending on site-specific situation (Koerner and Daniel, 1997).

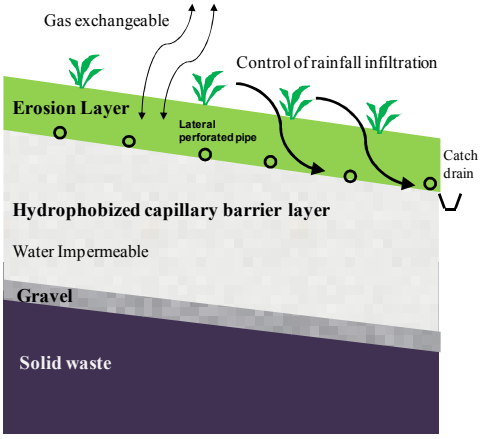

Figure 1 Schematic of hydrophobized capillary barrier layers.

The usefulness of HA application to enhance the degree of WR for soil grain samples were exemplified in Leelamanie and Karbu (2009a,b) and Bachmann and McHale (2009). The potential use of the induced soil-water repellency techniques in improving the performance of alternative cover system such as CB has been tested by Dell'Avanzi et al. (2010) who used sand mixed with polytetrafluorethylene (also known as Teflon) to improve hydraulic properties and seepage control ability in the CBs in laboratory experiments.

For developing the hydrophobized capillary barrier concept for landfill capping system this study investigated the potential use of the induced water repellency techniques in improving the performance of alternative capillary barrier capping system is an important aspect of the proposed concept. The three specific objectives of this study were (i) to assess WR characteristics of sands hydrophobized with hydrophobic agents such as OA and SA based on the measured contact angles, (ii) to develop a single, small-scale, high resolution mini T-TDR probe for simultaneous measurement of soil water potential and soil water content, and (iii) to assess the water retention characteristics for hydrophobic porous media under controlled wetting and drying cycles.

2. MATERIAL AND METHODS

2.1 Sample Preparation

Sand from Toyoura, Japan with a particle size range from 0.105 mm to 0.21 mm was used as the base material for preparing the mix of sand with hydrophobic agents (HAs). Prior to the HA-coating, the sand was washed with a low-foaming neutral cleansing agent, rinsed with distilled water several times, and air-dried. Cleaning helps to remove the dust and boost the adhesion bond between hydrophobic agent and sand (Israelachvili, 1991). Oleic acid (OA) (molar mass of 282.46 g mol^{-1}; Kanto Chemical Corporation, Tokyo, Japan) and stearic acid (SA) (molar mass of 284.48 g mol^{-1}; Kanto Chemical Corporation, Tokyo, Japan) were used as HAs in this study. The OA is a mono-unsaturated omega-9 fatty acid consisting of CH_3 and CH_2 groups, a carboxyl group (COOH) and a vinyl CH group (double bond CH=CH). The SA is a saturated fatty acid with 18 carbons with no double bonds, consisting of CH_3 and CH_2 groups and a carboxyl group (COOH). Both OA and SA are common organic acids found in various vegetable and animal sources (Gunstone, 2004).

Hydrophobized sand samples with different HA contents (in g HA per kg sand; g kg^{-1}) and different coating methods (mixing-in or solvent–aided) were used for the assessment of water repellency (WR). For the OA-coated samples, both the mixing and the solvent–aided methods were used. Sands were either mixed thoroughly with liquid OA in a plastic bag and stored at constant room temperature (20^{o}C) for 48 hours to equilibrate (mixing-in); or sands were immersed in a small container filled with OA-dissolved diethyl ether and kept in a draught vacuum chamber for three hours to allow volatilization of the diethyl ether. Thereafter, samples were stored for 48 hours at constant room temperature (solvent-aided).

Table 1 Requirements for capillary barriers in earthen cover systems. The items and descriptions summarized from Sharma and Reddy (2004), Simon and Műller (2004), and Benson and Khire (1995).

SN.	Items	Key points	Description
1	Site-specific	Use of locally-available materials	Construction materials are easily available in rural areas.
2	Low-cost	Less investment and maintenance cost	Use of available construction materials is proved to be cost effective.
3	Sustainable	Durable and long-term performance	design system performs well for controlling infiltration and surface water seepage for desired periods
4	Environmentally friendly	Use of environmental friendly materials and technologies	Construction materials are non-toxic and non-harm to human health and environment.
5	Engineered	Easy construction	Proposed system is easy to construct with locally available man-powers and skills.

After obtaining hydrophobized sand as described above, the samples were then prepared for the experiments through wetting and drying cycles. The coated sample was first packed in a cylindrical ring (5 cm in diameter and 1 cm height) at a dry bulk density of 1.58 g cm^{-3} (Table-2) and was saturated with distilled water using a hanging water column setup. Water was supplied from the bottom of the packed sample via a glass filter with a positive pressure of +1 cm. While wetting the samples, +1 cm slow water imbibition was maintained for 24 hours until the hydrophobized sand got fully saturated. Then the saturated sample was kept for 12 hours and after that drained at -30 cm hydraulic head. After cessation of drainage, the sample was removed from the cylindrical ring and stored at constant room temperature (20°C) for three days.

VAS was also sampled at 0 to 0.05 m depth from the forested hill-site at Fukushima in northeastern Japan, for calibration of newly developed mini T-TDR coil probe. Before the tests, the samples at field-water content (0.66 cm^3 cm^{-3}) were sieved gently through a 2-mm mesh screen (Kawamoto et al., 2007). Soil samples with different volumetric water content below field water content were obtained by drying at 60°C for different amount of time (0.25-24 h) followed by 48 h equilibration at 20°C room temperature. Air-dried samples were prepared by heating at 60°C for 24h in an oven and equilibrium at room temperature of 20°C. All the VAS samples used in this experiment were aggregated containing both intra-aggregate and inter-aggregate pores (Kawamoto et al., 2007). The soil organic carbon contents present in soil samples were measured by an automatic CN analyzer (CHN corder MT-5, Yanako, Kyoto, Japan).

2.2 Water Repellency Tests

The degree of WR of the samples was assessed with the water drop penetration time (WDPT) test, the molarity of ethanol droplet (MED) test, and the sessile drop method (SDM). Maximum recording time of WDPT was set to be 3600s in this study. For both contact angles (α_i from the MED test and α(t) from the SDM), higher values for the contact angles represent higher WR of the tested samples. Fig. 3 shows examples of recorded microphotographs for contact angles of 100° and 60°.

2.3 Mini T-TDR coil probe design and TDR equipment

In order to measure the ψ, a ceramic porous cup tensiometer 10 mm long, 6 mm outer diameter and 2 mm inner diameter was fixed to a 6-mm outer-diameter Perspex tube by an epoxy adhesive (Fig. 4). In the Perspex tube one millimeter away from the tensiometer end was peeled out to a depth of 0.5 mm, thereby making a 5-mm diameter and 20-mm long cylindrical depression on the tube. Following the work by Nissen et al. (1998) and Kawamoto et al. (2004a), a lacquered (quick-drying glue, Konishi company, Osaka) 0.3-mm diameter copper conductor wire was wrapped around a 5-mm diameter section of the Perspex tube. Four lacquered 0.3-mm diameter copper conductor wires were fixed on the coil at right angles. Conductor wires and four earth wires were soldered to a 50Ω thin coaxial cable. Nissen et al.(1998) revealed that use of four earth wires gave a satisfactory trace at all θ of interest for which both the beginning and end of the probe could be distinguished. A hollow cylindrical rubber stopper was fixed to the bottom of the tensiometer-coil probe assembly enabling the probe to be firmly fixed in the acrylic cylinder. The inner diameter of the Perspex tube was 4 mm throughout its length. The end of the tensiometer-coil probe was fixed to a coupling tube which enables attachment-detachment of a 4-mm diameter flexible tube. Finally, the coaxial cable was soldered to a 50 Ω BNC connector enabling the linkup between coil probe and cable tester (Tektronix 1502C, Tektronix Beaverton, OR). The waveform produced by the mini T-TDR coil probe when embedded in a medium was transferred from the cable tester to a personal computer through the RS232 serial port and analyzed by TACQ software (Evett, 1998). The parameters controlling resolution on the time axis were set on the cable tester as follows: velocity of propagation (V_P) = 0.61, distance per division (dist/div) = 0.05 m. The exact location of the beginning and end of the coil probe was identified following Nissen et al. (1998). The beginning of mini T-TDR coil probes is located before the first rise of the impedance (t_b), at the intersection between straight line and rising limb. The time (t_2) of the reflection signifying the end of the coil was determined by the intersection of a horizontal line drawn through the bottom of the distinct drop in plotted impedance before the second rising limb of the waveform and a line drawn tangent to the greatest slope of the second rising limb. The TACQ software was configured to above specification during the wave-form interpretation.

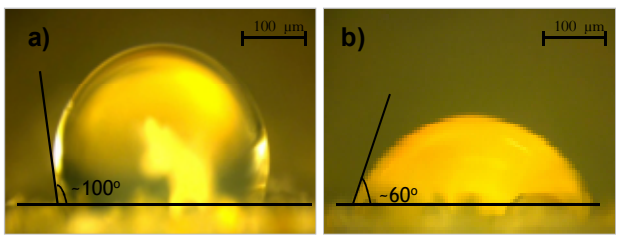

Figure 3 Microphotographs of OA (mixing-in) samples with a) 100° contact angles for t=0s and b) 60° contact angle for t=900s obtained from the SDM

2.4 Laboratory calibration

Calibration of the mini T-TDR coil probe was carried out by two different methods using a repacking method and a hanging water column method. In the repacking method, VAS (0 to 0.66 cm^3 cm^{-3} at approximately 0.02 cm^3 cm^{-3} intervals) and Toyoura sand (0 to 0.2 cm^3 cm^{-3} at approximately 0.02 cm^3 cm^{-3} intervals) were prepared with different water contents to measure the waveforms. VAS below 0.66 cm^3 cm^{-3} were obtained by drying the sieved soil in an oven at 60 ^oC for different periods followed by equilibrating for 48 h at 20 ^oC in sealed plastic bags. The soil-water contents of Toyoura sand below 0.2 cm^3 cm^{-3} were obtained by adding a known amount of distilled water to air-dried sand, mixing in a plastic bag and equilibrating for 48 h at 20^oC. The mini T-TDR coil probe was fixed to a transparent acrylic cylinder (20 mm height, 50 mm diameter, 2 mm thickness) through a hole in the side of the cylinder. The bottom of the ring was fixed to a 50-mm wide acrylic plate (Fig. 5a). The acrylic cylinder was divided into 5 layers to pack the soil samples uniformly. Soils were uniformly packed in the cylinder at constant dry bulk density (see Table 2) and T-TDR waveforms were obtained.

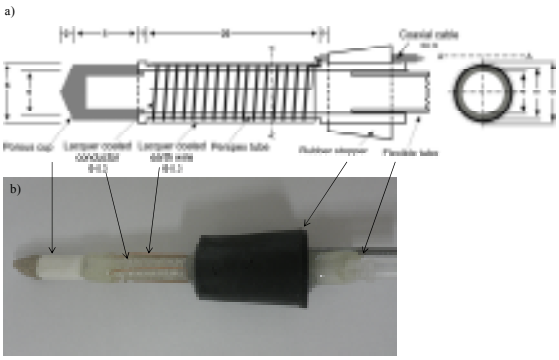

Figure 4(a) Schematic diagram and (b) a photograph of the mini tensiometer-TDR coil probe. All measurements are in millimeters.

In the hanging water column method, VAS (0.66 to 0.8 cm3 cm-3) and Toyoura sand (0.2 to 0.4 cm^3 cm^{-3}) were prepared with different water contents to measure the waveforms. A ceramic porous plate (glass filter) was placed at the bottom of the acrylic cylinder with a drainpipe at the bottom (Fig. 5b). The acrylic cylinder was marked into 5 layers to pack the soil samples uniformly. Air-dried Toyoura sand and field-water-content VAS samples were packed to a constant dry bulk density in the acrylic cylinder which was mounted with the coil probe with a saturated porous cup. The samples were then saturated with water under 0.1 MPa vacuum. The drainage was carried out by lowering the drainage pipe at desired water pressure head and recording the T-TDR waveforms. After draining, the samples were removed from the cylinder and dried in the oven at 105 ^oC to determine the volumetric water content and dry bulk density. The verification of volumetric water content and dry bulk density were done by calculating the mass of water driven off by drying and measuring mass of dry soil, respectively. For the 3-rod probe calibration, Toyoura sand were packed in a cylindrical polyethylene terephthalate container (inner diameter= 13 cm, height=25 cm) maintaining the constant dry bulk density. Calibration of conventional 3-rod probe was carried out by a repacking method.

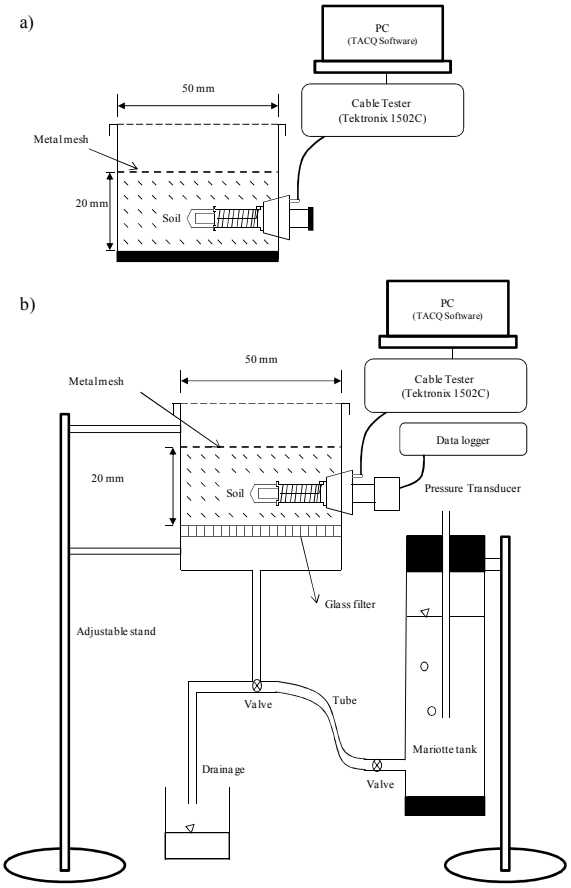

Figure 5 Experimental setup for calibration measuring soil-water content and soil-water potential using the (a) repacking method, and (b) hanging water column method.

2.5 Measurement of soil-water retention curve

For the estimation of soil-water retention curves, θ and ψ were simultaneously measured using a hanging water column equipped with a mini T-TDR coil probe 6 mm wide and 32 mm long. Toyoura sand samples with different hydrophobicities and VAS samples with different water contents were packed in an acrylic cylinder which was fitted with a saturated porous cup assembled with a mini T-TDR coil probe. A ceramic porous plate was placed at the bottom of the acrylic cylinder and connected by a flexible tube at the bottom to a drainage pipe and a Mariotte

tank (Fig. 5b). The porous cup at the tip of the mini T-TDR was saturated by injecting distilled water from the opposite end through a syringe, and connected to a pressure transducer through a short flexible tube. The pressure transducer was connected to a data logger (Campbell Scientific, CR10X) and then sequentially to a personal computer.

Water imbibition into the hydrophobic porous medium was imparted either by step-wise increments of water pressure (from -80 cm) (hereafter labeled as "step-wise imbibition") or a constant positive pressure (hereafter labeled as "constant positive imbibition") to evaluate the main wetting process. In the step-wise imbibition, the soil was slowly wetted from the bottom by opening the control valve below the suction chamber while maintaining a constant negative water pressure head using a Mariotte tank. The T-TDR readings and ψ were recorded continuously at one-minute intervals. Equilibrium was reached when readings became constant with the maintained water pressure head. Following the same step-wise procedure described above, the negative water pressure head was sequentially lowered and continued till a positive pressure head was reached (5 cm of H_2O for VAS; 0 cm H_2O for OA-coated samples; 2 cm H_2O for SA-coated samples). In the constant pressure imbibition, the packed sample was quickly wetted from the bottom by opening the control valve at the constant positive pressure of +15 cm. Similar to the step-wise imbibition method, T-TDR readings and ψ were recorded continuously at one-minute intervals. After the main wetting process, the Mariotte tank was disconnected and the drainage pipe connected to the glass filter. The drainage was carried out by lowering the drainage pipe to the desired water pressure head and the respective T-TDR waveforms were then recorded. For the main drying process, the samples were initially saturated with water under 0.1 MPa vacuum. The changes in θ and ψ in the drying processes were recorded at each desired pressure head.

3. RESULT AND DISSCUSSIONS

3.1 Initial Contact Angles for Hydrophobized Sands

α_i measured by the MED test and α(t = 0 sec) by the SDM (which is equivalent to initial contact angle α_i), as a function of HA content, are shown in Fig. 6, as are the measured WDPT values. The α_i values measured by the MED test were in good agreement with those measured by the SDM in the range of $\alpha_i > 90^o$ for each sample.

For OA-coated samples (mixing-in in Fig.6a and solvent-aided in Fig 6b), the measured α_i values increased sharply with increasing HA content and reached peak values of 101^o at 1.0 g kg^{-1} (mixing-in) and 97^o at 0.75 g kg^{-1} (solvent-aided). After the peak values, α_i gradually decreased with increasing HA content. Correspondingly, the WDPT values were highest at the peak values of α_i; at respectively 250 s for α_i = 101^o (mixing-in) and 52 s for α_i = 97^o (solvent-aided).

For SA-coated samples (solvent-aided in Fig. 6c), measured α_i values increased sharply to around 90^o and then gradually reached a maximum of 108^o at 6.0 g kg^{-1} HA. Measured WDPT values corresponding to $\alpha_i > 103^o$ for the SA-coated samples exceeded 3600s. Similar results for α_i were obtained for SA hydrophobized sands by Leelamanie and Karube (2009a, b). They observed that the α_i values exceeded 90^o at 1.0 g kg^{-1} HA (corresponding WDPT > 3600 s) and increased gradually up to α_i = 110^o at 5.0 g kg^{-1}, at which sand particles were considered to be fully coated with SA.

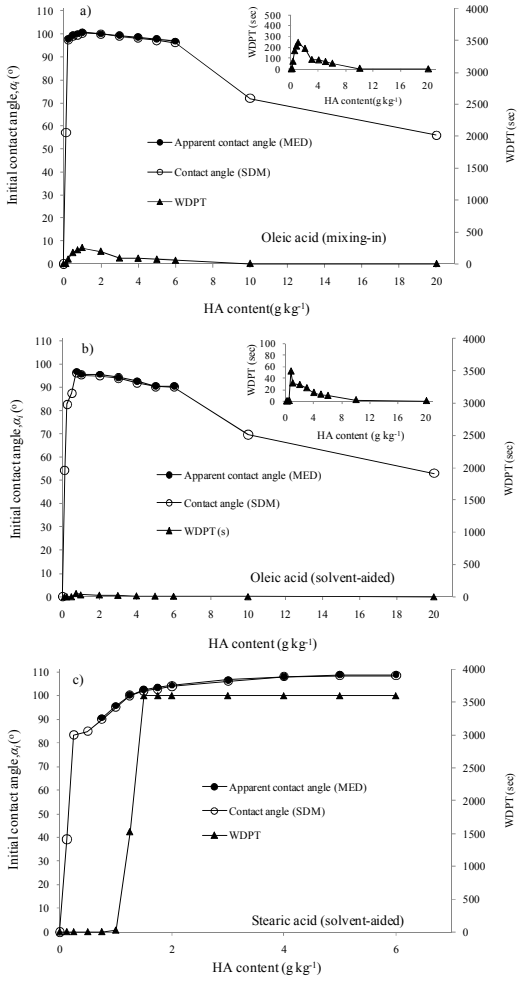

Figure 6 Initial contact angles, α_i, measured as a function of HA content by the MED test and the SDM for a) oleic acid (mixing-in), b) oleic acid (solvent-aided) and c) stearic acid (solvent-aided) samples. Results from the WDPT test are also shown. Note that the x-axis used in (c) is different from those in (a) and (b).

3.2 Time-Dependence of Contact Angles for Hydrophobized Sands

Observed time-dependence of contact angles, $\alpha(t)$, measured with the Sessile Drop Method (SDM) was plotted in Figure 7 for selected samples. Corresponding to the observed $\alpha(t)$ values, the temporal change in the surface free energy of the solids, γ_s (N m^{-1}), was also shown in the figure. Each test sample exhibited a gradual decrease in $\alpha(t)$ and a gradual increase in $\gamma_s(t)$, and reached an apparent equilibrium after 1200 and 1800s of the solid (grain)-water contact time for OA-coated samples (mixing-in and solvent-aided) and SA-coated samples (solvent-aided).

The reduction of contact angle (i.e., WR) with contact time can be mainly explained by adsorption of water molecules onto the grain-water contact surface and the consequent increase in surface free energy (Leelamanie and Karube, 2009a; Bachmann et al., 2007). In this study, the temporal change in $\alpha(t)$ was expressed by a simple exponential function,

$$\alpha = \alpha_i \exp(-At) \quad [1]$$

where α_i is the initial contact angle (^{o}) [$\alpha(t) = 0$ sec] and A is the coefficient of temporal change in the contact angle (i.e., temporal change in WR) (s^{-1}). Higher A value gives a higher decrease in the contact angle with time, representing a higher time-dependence of the contact angle (see Fig.8). Rearranging Eq. [2], the temporal change in γ_s can be expressed as,

$$\gamma_s = (2\Phi)^2(\gamma_L)(1+\cos\alpha)^2 \quad [2]$$

Fitting the measured $\alpha(t)$-plots with Eq. [1] using the measured α_i values, the A values were determined. The γ_s(t) values were subsequently calculated using Eq. [2] and the obtained A values. The $\alpha(t)$ and γ_s(t) curves well captured the temporal change in the contact angle and the surface free energy of the solids for all measurements (Fig.8). The fitted A values for all the tested samples are plotted in Figure 8 as a function of HA content. The A values for OA-coated samples (mixing-in) fluctuated widely within a range from 4×10^{-4} to 22×10^{-4} s^{-1} (Fig. 8a). The large fluctuation can be observed in the pretreated samples after the wetting and drying cycle. For the OA-coated samples (mixing-in), it is interesting that minimum A values were recorded at the HA content of 1.0 g kg-1, giving the peak values of α_i (=101^o) (Figs. 6a). On the other hand, the A values for solvent-aided OA- and SA-coated samples were relatively constant, ranging from 3×10^{-4} to 6×10^{-4} s^{-1}.

The results of calculating A values using the previously reported data for SA-coated samples (solvent-aided) in Leelamanie and Karube (2009a) are also given in Figure 8b. The A values reported in literature (Leelamanie and Karube, 2009a) were a little larger than our data, but exhibited only small fluctuations. This suggests that the solvent-aided samples are less time-dependent and exhibit higher WR persistence than the mixing-in samples.

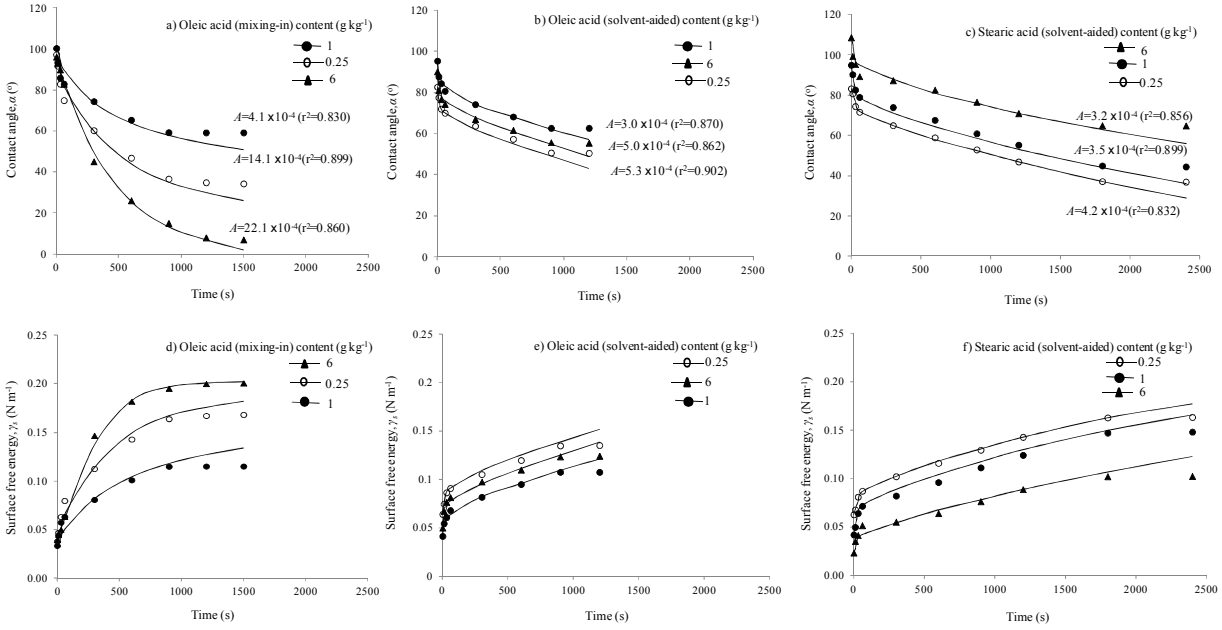

Figure 7 Contact angles, α, and soil surface free energy, γ_s, as a function of soil-water contact time for a) and d) oleic acid (mixing-in), b) and e) oleic acid (solvent-aided), and c) and f) stearic acid (solvent-aided) samples.

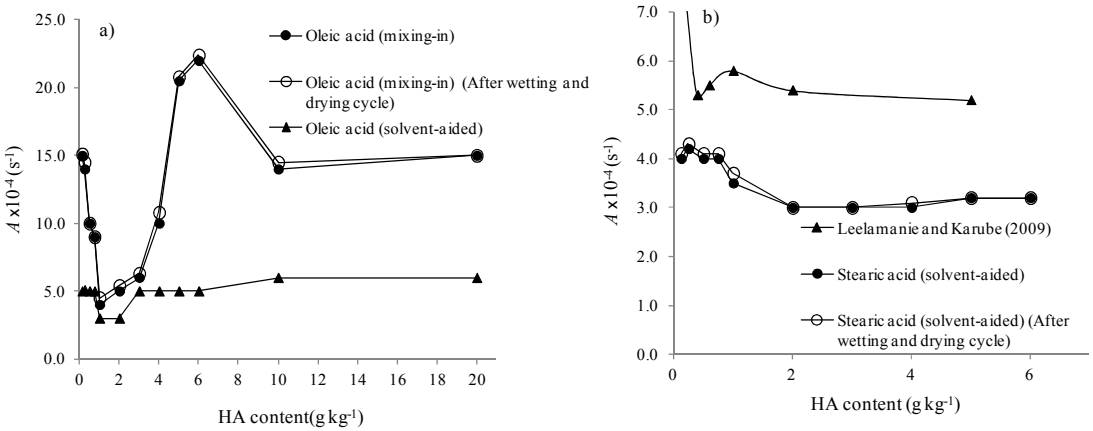

Figure 8 Effect of increasing hydrophobic agent (HA) on coefficient of temporal change in WR, A, in hydrophobized Toyoura sands before and after the wetting and drying cycle for a) OA (mixing-in) and OA (solvent aided) samples and b) SA (solvent-aided) samples. Note the different y axes.

3.3 Probe sensitivity experiment

There is a nonlinear ε-ε_{coil} relationship between the coil and reference probe caused by the contribution to ε_{coil} from the coil probe materials (Nissen et al., 1998). An alternative experiment was performed where differences in dielectric constant in the media under investigation did not exist and contact between TDR probes and calibration media was perfect to determine the correlation between the dielectric constant measured by a conventional three-rod TDR probe (ε) and mini T-TDR probe no. 5 (ε_{coil}). This was carried out by measuring the dielectric constant of known fluids (water, 99.9% ethanol, iso-propyl alcohol, acetone, phenyl ethanol, acetic acid, and castor oil) and air at a constant room temperature (20^{o}C). Besides the pure substances, different mixtures of ethanol and water were prepared, with 5 to 50% (v/v) water in ethanol, resulting in a total of fourteen different media. Measurement was done in a cylindrical polyethylene terephthalate container (inner diameter= 13 cm, height=25 cm). Probe and fluids were equilibrated to room temperature before the measurements were carried out. The dielectric constant was measured 5 times in each medium with both types of probes.

The developed mini T-TDR coil probes captured a wide range of dielectric constants from air to water (Fig. 9). The dielectric mixing model fitted well (RMSE=0.15, BIAS=0.1) with the measured ε-ε_{coil} relationship except at higher values with ethanol-water mixtures and water deviating from the mixing model. The discrepancy may partly be due to the lacquer coating and to errors introduced in determining the various values of ε_{coil} in mini T-TDR coil probe (Nissen et al., 1998).

3.4 Calibration for mini T-TDR coil probes

The calibration data of seven mini T-TDR coil probes for VAS and Toyoura sand are presented in Fig.10a and 10b. The measured ε_{coil} gradually increased with increases in θ for VAS and Toyoura sand. The coil probe captured well a wide range in θ from air-dry (θ_{dry}) to saturation (θ_{sat}) with a high accuracy for both materials. The seven probes did not follow a singular ε_{coil}-θ relationship. The measured ε_{coil} values for both soils were close in the soil-water content range 0.0 to 0.20 cm^3 cm^{-3}. The probe to probe variation may be due to variation in thickness of the lacquer coating on the waveguide (Nissen et al., 1998).

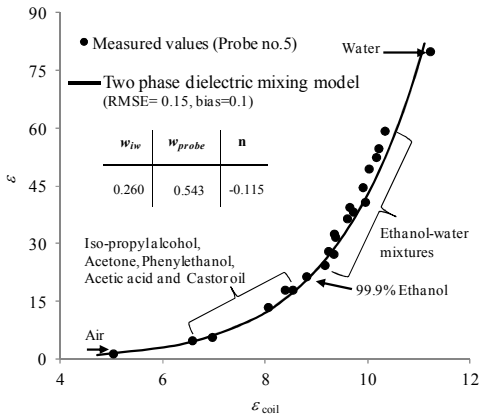

w_{iw}	w_{probe}	n
0.260	0.543	-0.115

Figure 9 Relationship between apparent dielectric constant measured with a conventional three-rod probe (ε) and a mini T-TDR coil probe (ε_{coil}) in air, water, ethanol, ethanol-water mixtures, iso-propyl alcohol, acetone, phenyl ethanol, acetic acid and castor oil. The solid line shows the two-phase dielectric mixing model fitted to the data points.

The third-order polynomial equation fitted to the normalized data (ε_{coil}-ε_{dry})-θ for VAS (RMSE=0.29, bias=0.032) and bare Toyoura sand (RMSE=0.98, bias=0.746) gave a reasonable fit (Figs. 10c and 10d). The best calibration method for individual TDR probes may be to use a soil-specific polynomial equation (Tomer et al., 1999; Stenger et al., 2007). However, one inherent

problem with the mini T-TDR coil probe is the necessity to carry out soil-specific calibration of individual probes due to the probe-to-probe variation. Applying dielectric mixing model curves (Fig. 10e and 10f) for the coil probes for VAS and Toyoura sand were obtained by substituting the fitted parameter *n, w* and α (for each soil) and using the average values of bulk density and porosity presented in Table 2. The dielectric mixing model underestimated volumetric water contents of the Toyoura sand in the wet region. Moreover, for VAS it underestimated the volumetric water content below 0.4 cm^3 cm^{-3} and overestimated above that. Although the dielectric mixing model showed less accuracy than the polynomial equations in Figure 10c, the estimation of the probe's dielectric value and partitioning factors provides valuable information that could be used to improve sensitivity and veracity of the T-TDR coil probe.

3.5 Development and validation of a new calibration model for $\varepsilon_{coil}(\theta)$

The dielectric mixing model, could not capture well the $(\varepsilon_{coil}-\varepsilon_{dry})-\theta$ relationship for both the wet and dry region in aggregated, and the wet region in single-grained soil. The VAS soil exhibited a unique "S" shape relationship for $(\varepsilon_{coil}-\varepsilon_{dry})-\theta$, and did not follow well the linear increase in the mixing model. Moreover, the normalized dielectric constant increased exponentially with soil-water content for Toyoura sand, but the mixing model showed a rather linear trend.

In this study a new calibration model for the relationship between the dielectric constant $(\varepsilon_{coil}-\varepsilon_{dry})$ and the volumetric water content (θ) is proposed (Fig. 11). The calibration model for aggregated soils is divided into two regions (region I & II), introducing $\theta_{critical}$ as the boundary between the intra- and inter-aggregate region with the intra-aggregate pore region from θ_{dry} to $\theta_{critical}$ and the inter-aggregate pore region from $\theta_{critical}$ to θ_{sat}.

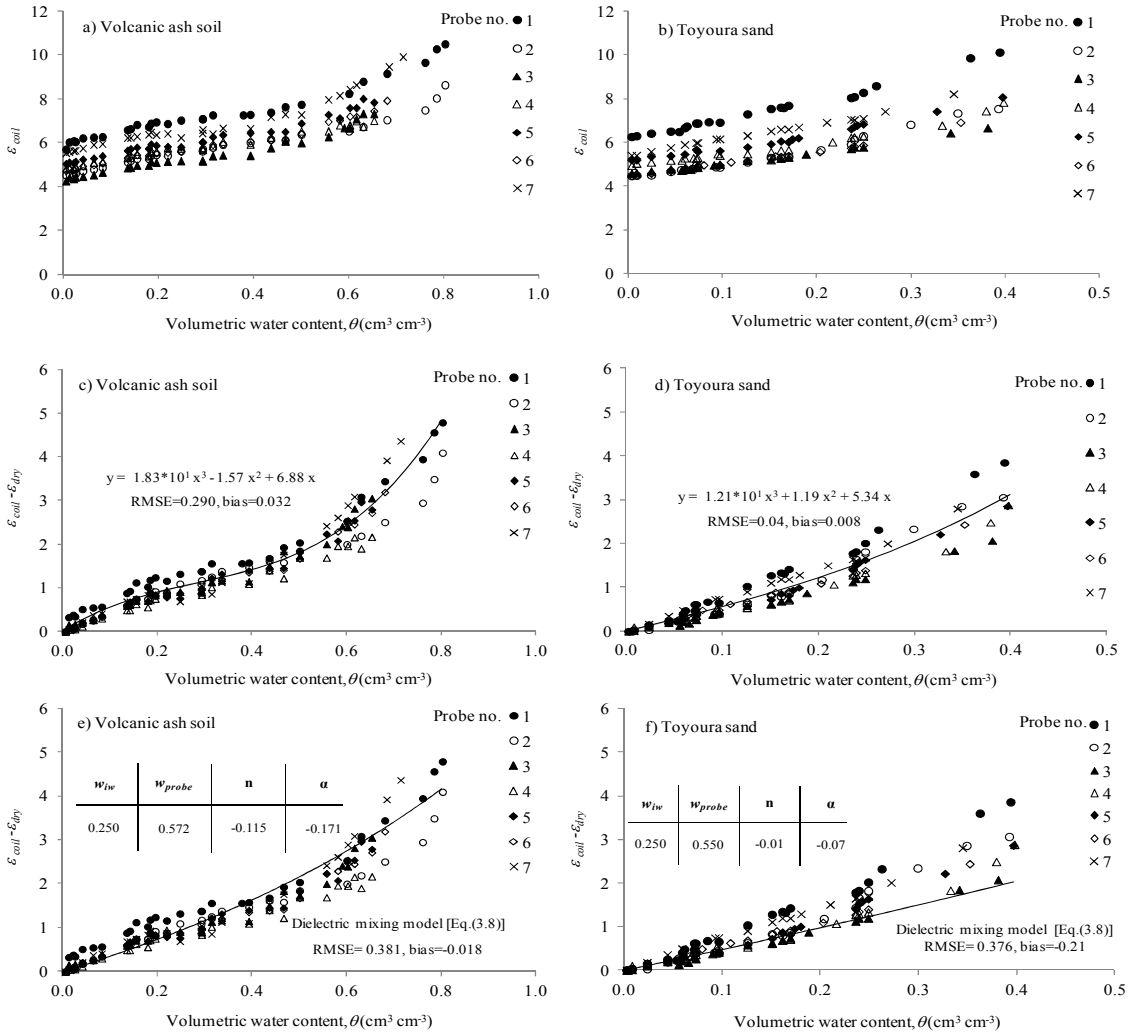

Figure 10 Relationship between dielectric constant, εcoil, and volumetric water content, θ, measured with seven mini T-TDR coil probes for volcanic ash soils (a), and bare Toyoura sand (b). Fitting of Polynomial expression and dielectric mixing model are shown in (c,d) and (e,f) in a normalized $(\varepsilon_{coil}-\varepsilon_{dry})-\theta$ relationship, respectively.

Table 2 Experimental materials and physical properties.

Soil	Soil particle density	Bulk density	Porosity	Soil organic carbon	Clay	Silt	Sand
	g cm^{-3}	g cm^{-3}	cm^3 cm^{-3}	%			
Volcanic ash soil	2.4	0.56	0.81	16.1	17.8	27.4	54.8
Toyoura sand							
Bare	2.64	1.58	0.40	0	0	0.1	99.9
1 g kg^{-1} OA	2.64	1.58	0.40	0.043	0	0.1	99.9
1 g kg^{-1} SA	2.64	1.58	0.40	0.059	0	0.1	99.9

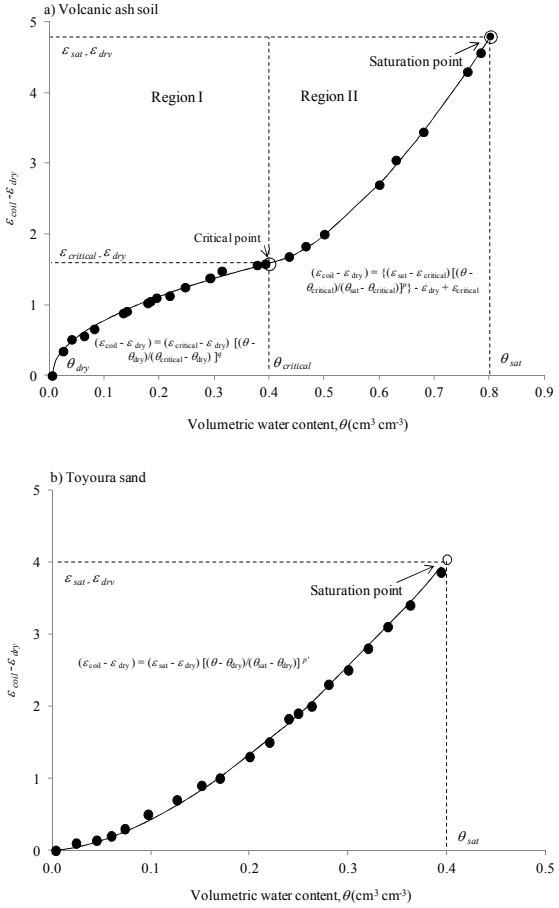

Figure 11 Illustration of proposed calibration model for (a) aggregated volcanic ash soil and (b) single-grained Toyoura sand to describe the relationship between the dielectric constant, ε_{coil}-ε_{dry}, and volumetric water content, θ.

Figure 12 illustrates the outcome of fitting the calibration model to the measured $(\varepsilon_{coil}-\varepsilon_{dry})$-$\theta$ data . Both calibration models were able to capture the $(\varepsilon_{coil}-\varepsilon_{dry})$-$\theta$ relationship. The empirical constants p, q and p′ of the fitting parameters for all seven mini T-TDR coil probes were p>1, q<1, and p′>1, respectively. The assumed critical point ($\theta_{critical}$ = 0.4 cm^3 cm^{-3}) in the calibration equation separated the two regions and well captured the unique "S"-shaped $(\varepsilon_{coil}-\varepsilon_{dry})$-$\theta$ relationship for VAS. The result revealed that the calibration model developed during this study performed better (RMSE=0.106 for VAS, RMSE=0.125 for Toyoura sand) than the dielectric mixing model (RMSE=0.324 for VAS, RMSE=0.33 for Toyoura sand) for both sand and VAS.

Typical soil-water retention curves (main drying process) for aggregated VAS and Toyoura sand obtained using mini T-TDR coil probe no. 2 equipped hanging water column method are shown in Figure 5b. The proposed calibration equations were used for the estimation of water content. The mini T-TDR coil probe captured the θ-pF relationship for a wide range of values from saturation (pF=0) to air-dried (pF=1.72 for Toyoura sand; pF=2.04 for VAS) (Fig. 13). The measured θ and ψ were compared with the soil-water retention curves (main drying process) obtained by Kawamoto et al. (2007, 2004b) for aggregated VAS and Toyoura sand using a hanging water column method, a pressure chamber and water potential meter and provided similar unimodal and bimodal van Genuchten model parameters when fitting the measured data. The mini T-TDR performed well in measuring θ_{coil} (RMSE=0.008, bias=0.0079) for volcanic ash soil. However, the coil probe seems to be slightly underestimating θcoil ($0.2<\theta_{coil}<0.3$) for Toyoura sand. The main reasons for the underestimation of θ may be due to the evaporation of soil water during the packing of the column and error introduced during the probe calibration procedure (Nissen et al., 1999).

3.7 Soil-water retention curves under wetting processes

The main wetting curves during the step-wise and constant positive imbibitions are plotted in Fig. 14. OA- and SA-coated Toyoura samples showed a sharp increase in θ from initial water content to almost full saturation with a slight increase of ψ in the wetting process. The θ increments for these samples were steeper than for the water-adjusted hydrophobized Toyoura sand samples (Fig. 14).

3.6 Soil-water retention properties under repeated wetting and drying cycles

Simultaneous measurements of θ and ψ during the step-wise imbibition process of the repeated wetting and drying experiments for water-repellent soils using the hanging water column method are plotted in Fig. 15 for selected samples. The maximum water-holding capacity of the soil in different treatments is a function of total pore volume (Jury et al., 1991).

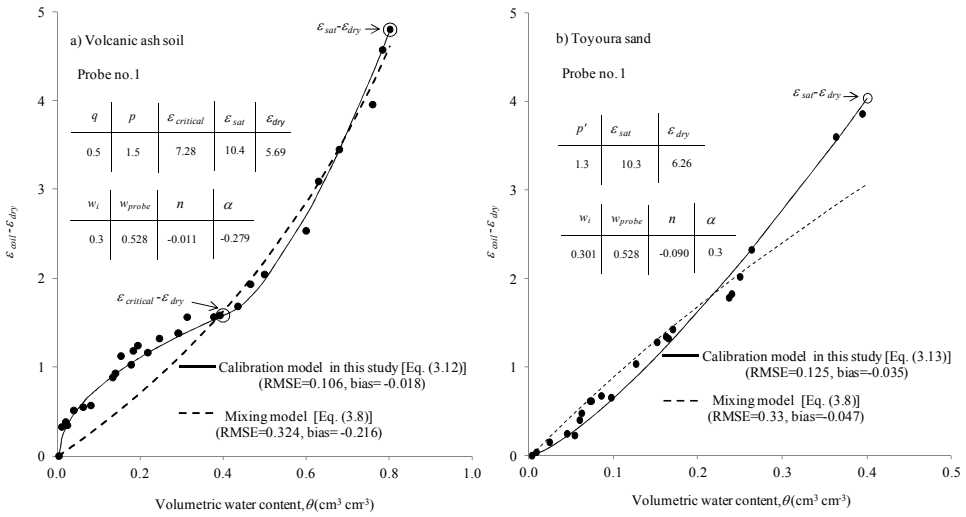

Figure 12 Calibration model fitted to the normalized dielectric constant, ε_{coil}-ε_{dry}, and volumetric water content, θ, relationship measured with mini T-TDR probe no. 1 for (a) volcanic ash soil and (b) Toyoura sand.

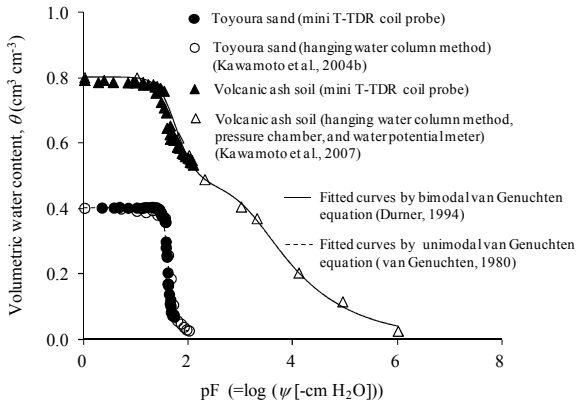

Figure 13 Soil-water retention curves for volcanic ash soil and bare Toyoura sand. The θ_s values are plotted at pF=0.

4. CONCLUSION

Sands hydrophobized by OA and SA revealed good performance evaluated by measured contact angle and hydraulic properties (soil-water retention curves), implying a good potential for using this techniques in capillary barrier systems.

The hydrophobic organic matter content was found to be the important factor affecting WR. For solvent-aided and mixing-in OA coated samples, α_i sharply increased with increasing HA content to reach peak values of 97° to 101° at 0.75 to 1 g kg^{-1} HA and gradually decreased after that. The WDPT and contact angle, for solvent aided SA-coated samples increased with increasing additions of HA to reach the maximum α_i =108° at 6 g kg^{-1} HA. The contact angle decreased exponentially with the soil-water contact time and reached an apparent equilibrium depending on HA contents. The newly developed exponential function well captures the time dependence of the contact angle.

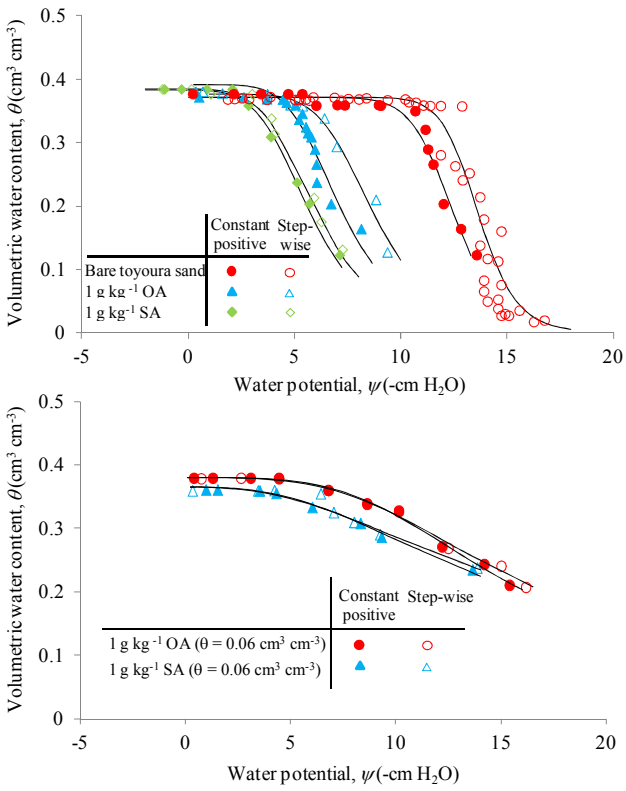

Figure 14 Main wetting curves during step-wise and constant positive pressure imbibition for a) bare (air-dried), OA- and SA- coated Toyoura sand samples (1 g kg^{-1}), and b) OA- and SA-coated Toyoura sand samples (1 g kg^{-1}) with 4% initial-water adjusted (θ_i = 0.06 cm^3 cm^{-3}). Symbols show measured wetting data and solid lines show curves fitted by the VG (1980) model.

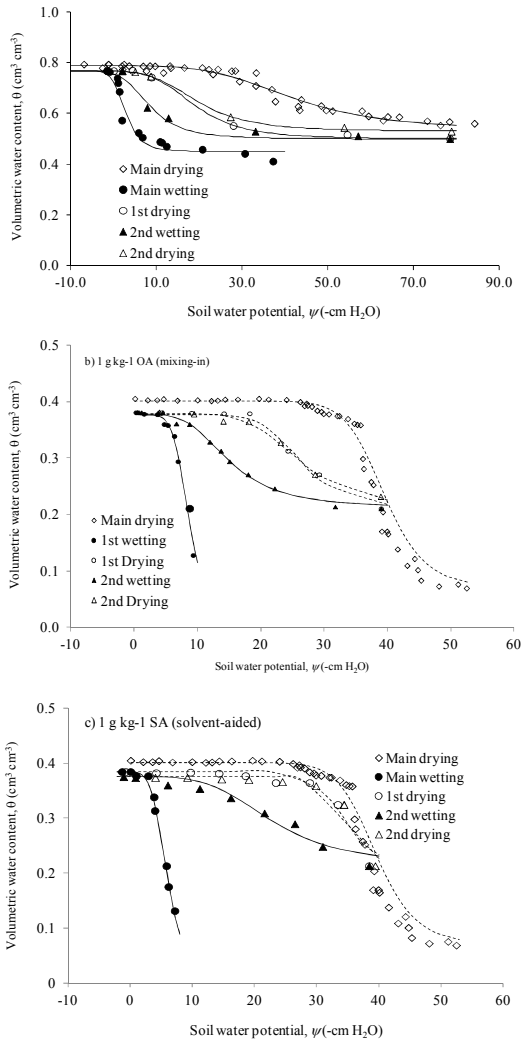

Figure 15 Volumetric water content, θ, as a function of water potential, ψ, for (a) VAS (air-dried), (b) OA-coated, and (c) SA-coated Toyoura sand samples (1 g kg^{-1}).

A mini T-TDR coil probe was developed for the measurement of soil-water retention properties of bimodal and unimodal water-repellent soils. The new mini T-TDR probe thereby seems highly useful for obtaining simultaneous, small-scale (point-like) measurements of water content and matric potential in unsaturated porous media hereunder will facilitate investigating the effects of water repellency on water retention properties. A subsequent study will further investigate the water retention properties of uni- and bi-modal media at different degrees of WR, applying the new small-scale T-TDR coil probe. The new calibration model for the mini T-TDR coil probe described well the $(\varepsilon_{coil}-\varepsilon_{dry})-\theta$ relations for both sand and VAS.

WR had a direct and predictable effect on the soil-water retention curves, and affect the shape of the wetting front. The mini T-TDR coil probe showed the excellent performance in measuring controlled repeated wetting and drainage curves in hydrophobic and hydrophilic media.

9. REFERENCES

Albright, W.H., Benson, C.H., Gee, G.W., Abichou, T., Roesler, A.C., and Rock, S.A., (2003) "Examining the alternatives," *Civil Eng*ineering, 73(5), pp. 70-74.

Bachmann, J., and McHale, G.. (2009) "Superhydrophobic surfaces: a model approach to predict contact angle and surface energy of soil particles,"*European Journal of Soil Sciences*, 60, pp. 420-430.

Bachmann, J., Deurer, M., and Arye, G., (2007) "Modelling water movement in heterogeneous water- repellent soil: 1. Development of a contact angle-dependent water-retention model," *Vadose Zone Journal*, 6, pp. 436-445.

Benson, C., and Khire, M., (1995) "Earthen covers for semi-arid and arid climates," In R.J. Dunn and U.P. Singh. (ed.) *Landfill Closures Environmental Protection and Land Recovery*, ASCE, GSP No. 53, pp. 201-217.

Dell'Avanzi, E., Guizelini, A.P., da Silva, W.R., and Nocko, L.M., (2010) "Potential use of induced soil-water repellency techniques to improve the performance of landfill's alternative final cover systems," In Buzzi et al. (ed.) *Unsaturated Soils, Two Volume Set: Experimental Studies in Unsaturated Soils and Expansive Soils*, **V. 1**, CRC Press, Boca Raton, FL., pp. 461-466.

Gunstone, F.D., (2004) "*The chemistry of oils and fats: Sources, composition, properties and uses,*" Blackwell Publishing Ltd. CRC Press. Boca Raton, FL.

Israelachvili, J., (1991) "*Intermolecular and surface forces*," 2nd ed. Academic Press, San Diego.

Jury, W.A., Gardner, W.R., and Gardner, W.H., (1991) "*Soil Physics*," 5th ed. John Wiley & Sons, New York.

Kawamoto, K., Moldrup, P., Komatsu, T., de Jonge, L.W., and Oda, M., (2007) "Water repellency of aggregate-size fractions of a VAS," *Soil Science Society of American Journal*, 71, pp.1658–1666.

Kawamoto, K., Moldrup, P., Komatsu, T., and Oda, M., (2004a) "Estimating soil water characteristic curves of water repellent volcanic ash

soils by time domain reflectometry coil probe measurements," *Trans. of JSIDRE*, 233, pp. 83-91.

Kawamoto, K., Mashino, S., Oda, M., and Miyazaki, T., (2004b) "Moisture structures of laterally expanding fingering flows in sandy soils," *Geoderma*, 119, pp.197–217.

Koerner, R.M., and Daniel, D.E., (1997) "*Final covers for solid waste landfills and abandoned dumps*," ASCE Press, New York.

Leelamanie, D.A.L., and Karube, J., (2009a) "Time dependence of contact angle and its relation to repellency persistence in hydrophobized sand," *Soil Science Plant Nutrition*, 55, pp. 457-461.

Leelamanie, D.A.L., and Karube, J., (2009b) "Effects of hydrophobic and hydrophilic organic matter on the water repellency model sandy soils," *Soil Science Plant Nutrition*, 55, pp. 462-467.

Nissen, H.H., Moldrup, P., and Henriksen, K., (1998) "High-resolution time domain reflectometry coil probe for measuring soil water content," Soil *Soil Science Society of American Journal*, 62, pp.1203–1211.

Nissen, H.H., Moldrup, P., de Jonge, L.W., and Jacobsen, O.H., (1999) "Time domain reflectometry coil probe measurements of water content during fingered flow," *Soil Science Society of American Journal*, 63, 493–500.

Sharma, H.D., and Reddy, K.R., (2004) "*Geoenvironmental Engineering: Site Remediation, Waste Containment, and Emerging Waste management technologies*," John Wiley & Sons, Hoboken, New Jersey.

Simon, F.G., and Müller, W.W., (2004) "Standard and alternative landfill capping design in Germany," Environmental Science Policy, 7, pp. 277–290.

Stenger, R., Wöhling, T., Barkle, G.F., and Wall, A., (2007) "Relationship between dielectric permittivity and water content for vadose zone materials of volcanic origin," *Australian Journal Soil Research*, 45, pp. 299-309.

Stormont, J.C., (1995) "The effect of constant anisotropy on capillary barrier performance," *Water Resources Research*, 31, pp. 783-786.

Tomer, M.D., Clothier, B.E., Vogeler, I., and Green, S., (1999) "A dielectric-water content relationship for sandy volcanic soils in New Zealand," *Soil Science Society of American Journal*, 63, pp.777–781.

van Genuchten, M.Th., (1980) "A closed-form equation for predicting the hydraulic conductivity of unsaturated soils," *Soil Science Society of American Journal*, 44, pp.892-898.